Self-testing of analog parts terminated by ADCs based on multiple sampling of time responses

Zbigniew Czaja

Gdansk University of Technology,

Faculty of Electronics, Telecommunications and Informatics,

Department of Metrology and Optoelectronics,

ul. G. Narutowicza 11/12, 80-952 Gdansk, Poland, phone: ++48 58 347-14-87,

fax: ++48 58 347-22-55, email: zbczaja@pg.gda.pl.

Abstract— **A new approach to self-testing of analog parts terminated by ADCs in mixed-signal electronic microsystems controlled by microcontrollers is presented. It is based upon a new fault diagnosis method using a transformation of the set of voltage samples of the time response of a tested analog part to a square impulse into localization curves placed in a multi-dimensional measurement space. The method can be used for fault detection and single soft fault localization. Modified Digital Fourier Transform formulae are used for conversion of the measurement results to the form used by the fault detection and localization algorithm during the self-testing of the system and also for creation of the fault dictionary. The results of experimental verification of the approach are included in this paper.**

Index Terms – Microcontrollers, Fault diagnosis, Analog circuits, Fourier transforms, Self-testing.

I. INTRODUCTION

At present, almost all electronic devices are produced as electronic embedded systems, that is, as systems with an "embedded intelligence". These systems are applied in almost all spheres of human activities, for instance, in motorization, medicine, automation, telecommunication, multimedia etc.

An important group of these systems is mixed-signal electronic microsystems (for example, applied in metrology, medicine and in automation). They consist of a digital part serving to control and process data and an analog part usually used to adapt (by preliminary conversion) signals coming from analog sensors. Moreover in many cases these systems are controlled by microcontrollers.

An important and desirable feature of electronic embedded systems is their reliability, which can be achieved by among others implementation of self-testing procedures in these systems. The procedures deal with functional testing of a whole system [1], a software [2,3] and its respective blocks [4].

For mixed-signal microsystems the self-testing procedure contains testing of a digital part (hardware and software) and, what we have to underline, testing of an analog part.

There are a few groups of methods of testing of analog parts, especially for analog filters and amplifiers: based on sigma-delta modulators [5,6], based on the oscillation-test methodology [7,8], utilizing a test strategy using power spectral analysis [9] and based on BISTs dynamically configured with internal resources of microcontrollers controlling these microsystems [10-13].

Therefore, a new method of testing of analog parts of these systems generalizing the method presented in [14] is proposed in the paper. It is based upon the new fault Simulation Before Test (SBT) diagnosis method which uses the transformation converting the set of voltage samples of the time response of a tested analog part to a square impulse into a measurement point, that is into a set of coordinates defined by the measurement space. This point is used together with a family of localization curves (the set of signatures of the fault dictionary of the tested analog circuit) placed in the multidimensional measurement space by the fault detection procedure and by the single soft fault localization procedure. The transformation is based on modified DFT (Digital Fourier Transform) formulae. Thanks to the proposed modification, the computational complexity of the method is small. Hence, the measurement and diagnosis procedures can be realized by simple 8-bit microcontrollers generally used in practice (for instance, the AVR family, the PIC family).
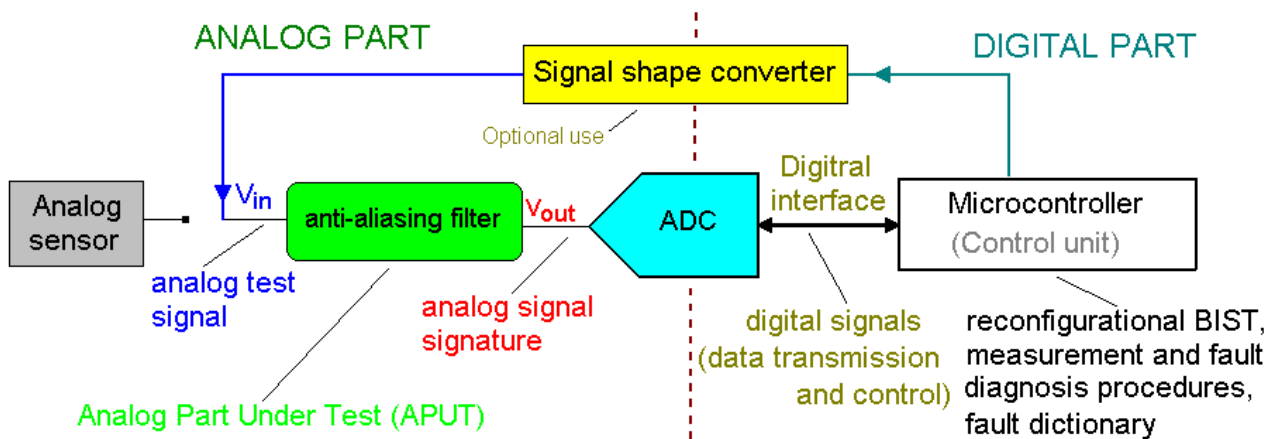

Figure 1. The mixed-signal microsystem in the self-testing mode

Moreover, we consider that it is not necessary to extend the system with additional components to execute the self-test. The square impulse test waveform that is applied to the Analog Part Under Test (APUT) is generated within the microcontroller (digital inputs and timers) and the voltage samples of the time response of the APUT are acquired using the existing system ADC, which is one of the novel features of this approach as proposed in [10-13]. Optionally, we can use a very simple circuit called a signal shape converter (Fig. 1) which improves parameters of signals generated by the microcontroller.

2

II.   THE SELF-TESTING APPROACH OF ANALOG PARTS

Because the proposed self-testing approach is based on the SBT method, it consists of two parts:

- A pre-testing part where the fault dictionary of the APUT is generated and stored in the program memory of the microcontroller. This part is realized during the system design and only once for a given analog part in a simulated way on a PC computer.

- A testing part run by the microcontroller for instance, after initialization of the system to verify the correct work of the APUT.

The second part is divided into two stages, the first one realized according to the measurement procedure, the second one according to the detection and localization procedures.

A.   The hardware solution

An implementation of the self-testing approach was illustrated on the example of the microsystem based on the ATmega16 microcontroller [15] and the 16-bit ADC AD7694 [16] controlled via the SPI interface (Fig. 2). The ATmega16 has the following peripherals required by the method: two 8-bit timers and one 16-bit timer. They enable to generate square impulses with programmable duration times and to precisely measure time (the time resolution is equal to 0.25 μs for a 4 MHz quartz crystal oscillator of the microcontroller).

In the main mode the analog signal v_{in} coming, for instance, from sensors is transmitted and filtered by the APUT, and next sampled by the Voltage Measurement Block (VMB), which consists of the external 16-bit ADC and internal devices of the microcontroller (Fig. 2). The 16-bit timer is responsible for synchronization of the ADC triggering – controlling the CNV signal, and the SPI interface for communication between the microcontroller and the 16-bit, charge redistribution, successive approximation ADC.
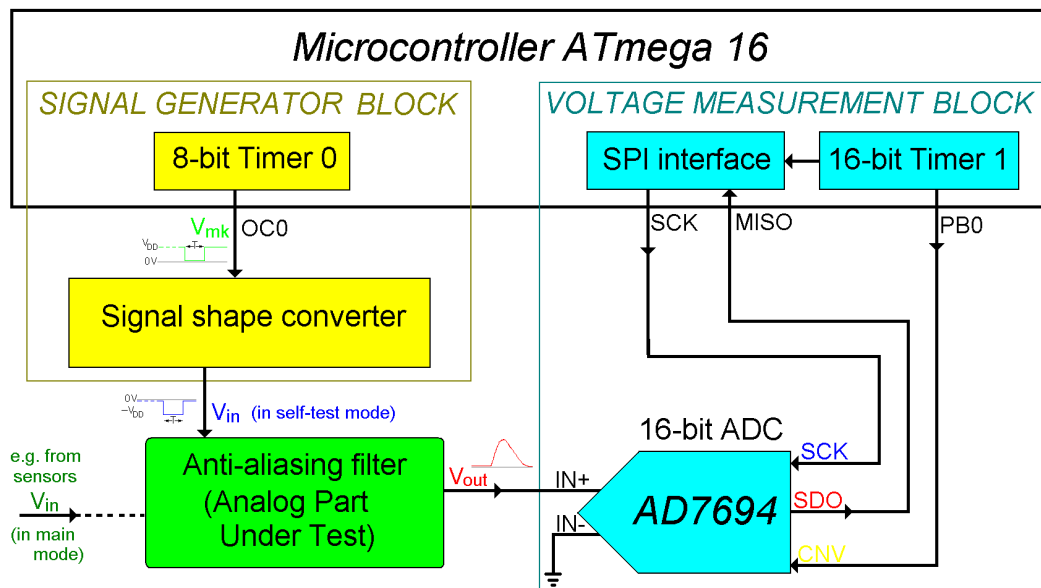

Figure 2. The mixed-signal microsystem based on the ATmega16 in the self-testing mode

3

In the testing mode the signal coming from sensors is disconnected and replaced by the testing signal v_{in} with known parameters (a single square pulse with the amplitude set to $-V_{DD}$ (the negative supply voltage) and with a programmable duration time T). This signal is generated by the Signal Generator Block (SGB), which consists of the 8-bit timer of the microcontroller and, if it is required by the APUT, the Signal Shape Converter (SSC). Hence, the SGB is configured from internal devices of the microcontroller only during the testing procedure. Therefore, the implementation of the self-testing procedure needs extension of the system only by one simple block (the SSC). The remaining blocks change their function in a programmable way in the testing time.

For illustration of the method, a second order low-pass filter with the multiple feedback (MFB) topology was chosen as the APUT (Fig. 3). It can seem that we have chosen as an example a narrow class of analog circuits (anti-aliasing filters), but these circuits are commonly applied in engineering practice. In the modern era of digital circuits, engineers prefer to use the simplest analog circuits possible, and only where necessary, to reduce costs. Because the MFB filter inverts the input signal, and the 16-bit ADC can measure only positive voltages, we have to use the SSC. It inverts the square impulse generated on the OC0 pin of the microcontroller. Thanks to this, the APUT response is positive and directly measurable by the 16-bit ADC.

Obviously, for filters based on the Sallen-Key topology the SSC is unnecessary [10-12], which further simplifies the SBG.
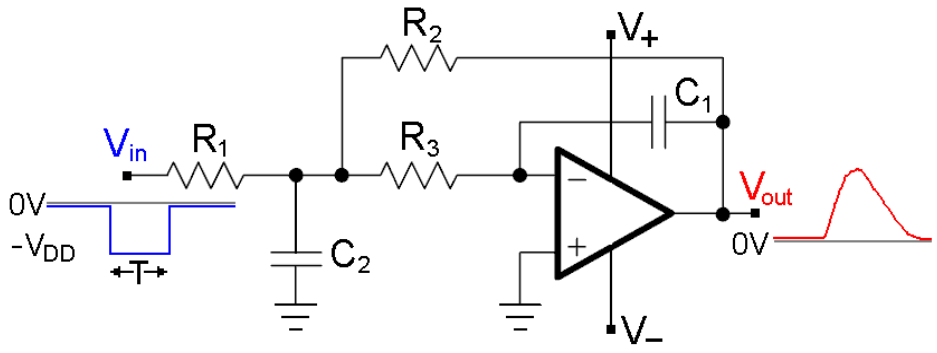

Figure 3. The second order low-pass filter based on the multiple feedback topology as an example of the APUT ($R_1 = 15401\ \Omega$, $R_2 = 15403\ \Omega$, $R_3 = 3481\ \Omega$, $C_1 = 10.028$ nF, $C_2 = 47.057$ nF)

The SSC is built with only two IRF7105PBF [17] chips in a SO-8 package and two resistors, as shown in Fig. 4. The resistors work as a voltage divider. The values of the resistors were established taking into account the fact that the voltage on the output of the voltage divider, when the first transistor is off, should be smaller than the gate threshold voltage (–3.0 V). Hence, the SSC is simple, that is, it is cheap in an application and it occupies a small board space. It also follows from the fact that we use the negative supply voltage existing in the system, that is, in our case, the negative supply voltage of the amplifier.
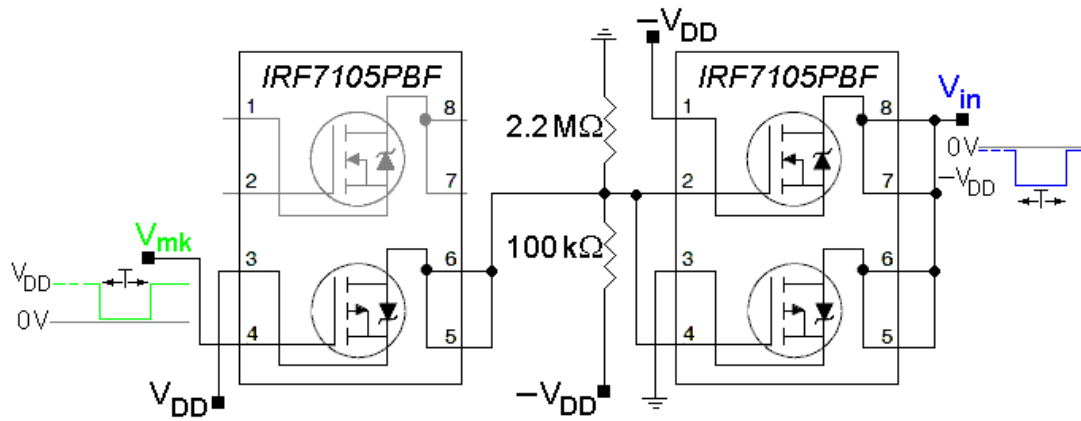
Figure 4. The signal shape converter consisting of three MOSFET transistors and two resistors

Additionally, the SSC eliminates the influence of electrical parameters (especially the output pin impedance depending on the pin sink current [15]) of the OC0 output pin of the microcontroller, which in special cases can influence the difference between measurement results and simulation results, as affirmed in [18-20]. It follows from the fact that the IRF7105PBF consists of two HEXFET power MOSFETs, the first one with an N-channel and the second one with a P-channel. They have small values of the static drain-to-source on-resistance (0.1 Ω and 0.25 Ω) and a high value of continuous drain current (3.5 A and –2.3 A respectively).

B. *The measurement procedure*

In the testing mode the APUT is stimulated by a square pulse v_{in} with the amplitude set to $-V_{DD}$ and the duration time $T = 196$ μs determined by the 8-bit Timer 0 (Fig. 5). The APUT response is sampled N times in equal time distance t_s by the external 16-bit ADC AD7694 controlled via the SPI interface (the clock line SCK and the data output line SDO – as shown in Fig. 2). The CNV line is used to start the ADC conversion. The voltage reference of the 16-bit ADC is set to V_{DD}. We assumed that the time distance t_s between next samples is equal to T_a/N, where T_a is the acquisition time and it is set to $10T$. Hence, we collect N 16-bit binary data $\{v_n\}_{n=1,...,N}$ representing voltage samples. They are stored in successive integer type variables $V(n)$, where $n=1,.., N$.
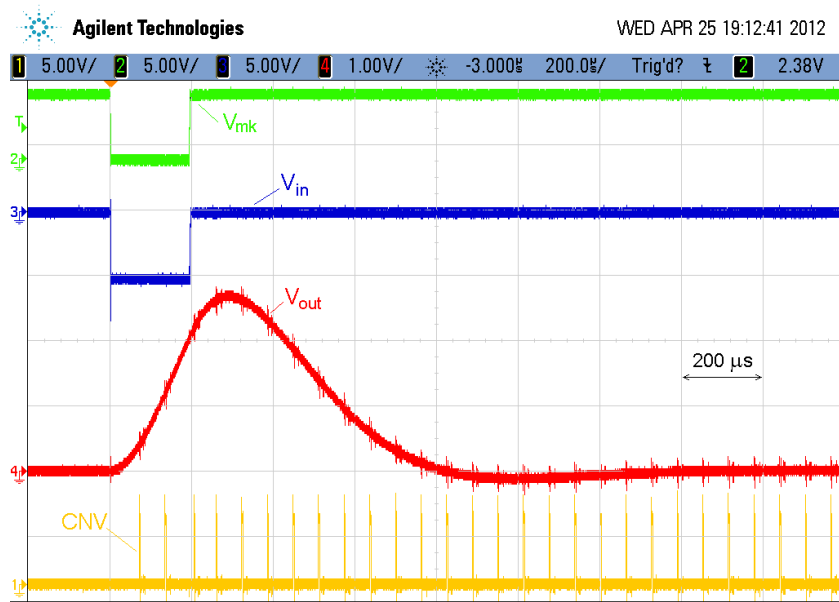
5

Figure 5. Timings of the stimulation square impulse and the time response of the APUT during the measurement procedure (observed by the MSO7054B oscilloscope)

Hence, as it is shown on Fig 5 and it is implemented in the measurement function [14] (Fig. 6), we start to measure N voltage samples of the time response of the APUT by the external ADC (the CNV signal) simultaneously with generation of the single square pulse v_{mk} at the OC0 output of the microcontroller. We use the overflow of the Timer 1 for synchronization of the sample voltage triggering. It occurs at time intervals equal to $t_s = 10T/N - t_d$ (t_d – correction following from software delays). The duration time T is determined by the Timer 0 Compare Match Interrupt. The SSC shifts the v_{mk} pulse about $-V_{DD}$ to obtain the negative pulse v_{in}.

The measurement of a single voltage sample is executed by the spiADC function. It controls the conversion of the external ADC and it reads the measurement result via the SPI interface.

From the timings generated by the spiADC function (Fig. 7) it is seen that we start the ADC conversion by setting the CNT line by about 3 µs to initiate the conversion. Next we read the result from the ADC deriving on the SDO line by two writings to the SPDR register of the SPI controller – two eight-impulse sequences on the SCK line.
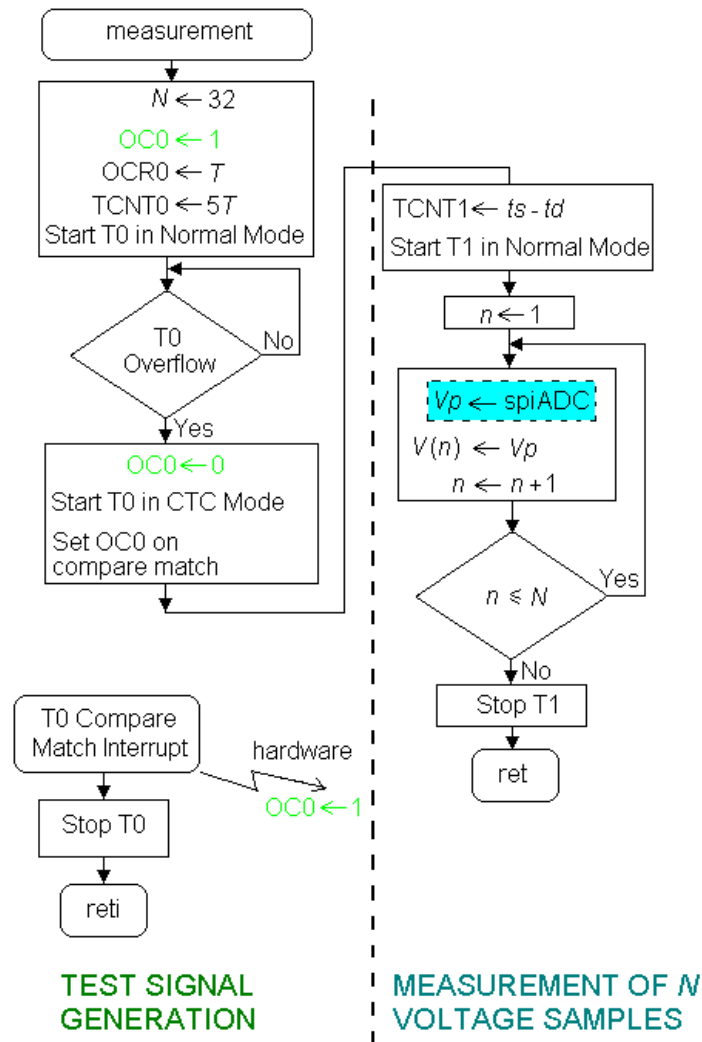
Figure 6. An algorithm of the measurement procedure which measures N voltage samples implemented in the measurement function
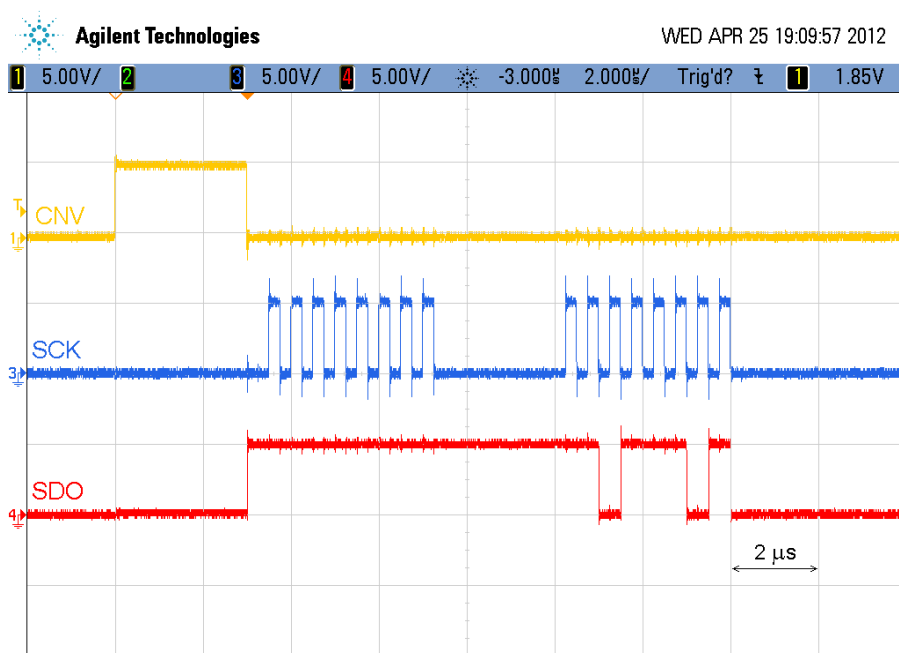

Figure 7. Timings of the SPI communication between the microcontroller and the external ADC (observed by the MSO7054B oscilloscope)

The algorithm of the spiADC function is shown in Fig. 8. The function consists of the part running in the main loop and the part implemented in the overflow of the Timer 1 interrupt service. In the main loop we set the the *end_conv* variable and wait for its clearing. In the interrupt service we start the ADC conversion, we read data from the ADC and at the end we clear the *end_conv* variable used to program synchronization between the main function and the interrupt service. That is, we can say that the SPI in a hardware way realizes triggering the conversion and reading of the measurement result from the external ADC.
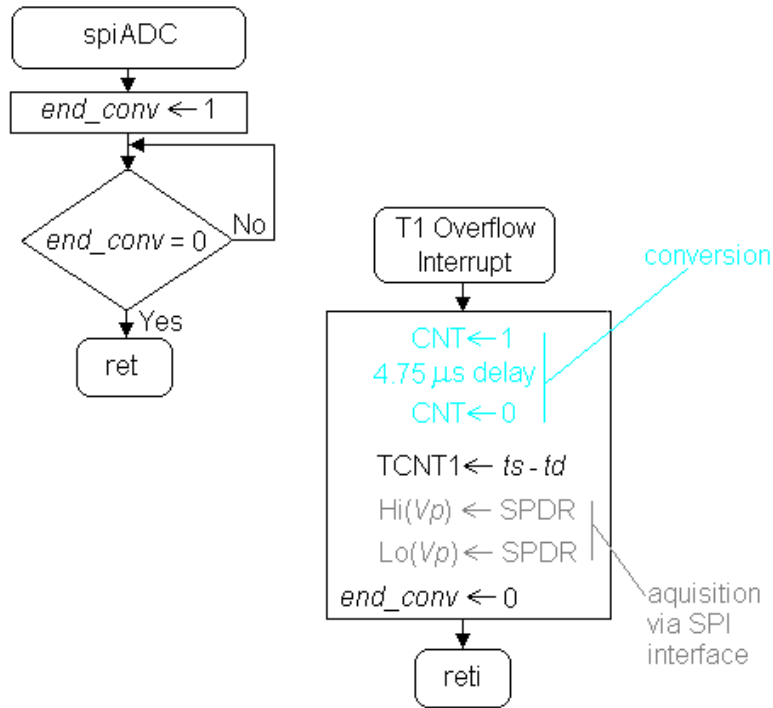

Figure 8. An algorithm of the spiADC function which measures a single voltage sample of the time response of the APUT

C. The fault dictionary

When stimulated by a single square pulse, the time response of the TAP depends upon the number of its components, p_i, where ($i = 1,.., I$), and the range of values that p_i can take. In the TAP (Fig 3) $I = 5$, and a range of non-overlapping set of values $0.2\ p_{inom}$ to $5\ p_{inom}$ has been assumed; where p_{inom} is the nominal value of the ith component (Fig. 9). That is, we can distinguish them in the same way as presented in [10-12]. Obviously, it is fulfilled for an assumption of existence of only single soft faults in the APUT. Therefore, distinction and assignation of subsets of these responses to respective components is possible – a fault localization, and also given response from the subset to a specific value of the component – a fault identification.
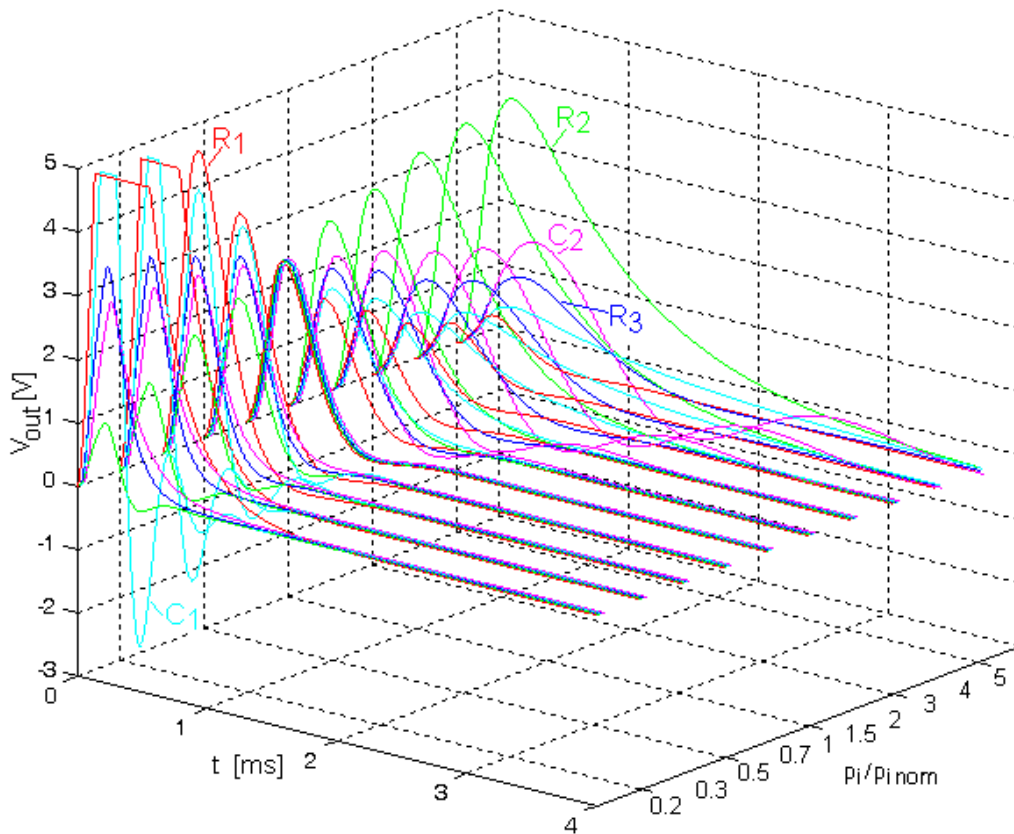
Figure 9. Timings of time responses of the APUT for different values of its components

Hence, the fault dictionary for single soft faults can consist of data describing the set of all possible time responses of the APUT. For example, if each time response is described by $N = 32$ 16-bit samples (2 bytes), and it is generating $J = 64$ time responses for each component (for J values of a component included in the assumed range), the size of the fault dictionary will be equal to $2NJI = 2 \cdot 32 \cdot 64 \cdot 5 = 20\,480$ bytes. It is not acceptable for small 8-bit microcontrollers, because the typical size of their program memory is 4 kB, 8 kB, 16 kB, 32 kB, seldom 64 kB and 128 kB.

For this reason, the fault dictionary should consist only of those unique features of the time responses that allow unambiguous localization of single soft faults, to keep the memory requirement to a minimum.

Thus, a new approach is proposed: "compressing" the fault dictionary $\{\{\{v_{n,j,i}\}_{n=1,...,N}\}_{j=1,...,J}\}_{i=1,...,I}$ to the new data set represented by I localization curves placed in a K-dimensional space [14]. Each curve (Fig. 10) is traced from J points, and each point is described by K coordinates. Therefore the i-th curve represents changes of properties of the APUT following from changes of i-th component values: $\{p_{j,i}\}_{j=1,...,J}$.

Thanks to this approach, the size of the fault dictionary is N/K times smaller and for the investigated example (we assumed a 4-dimensional measurement space – $K = 4$) it is equal to 2560 bytes, what is acceptable for microcontroller systems.
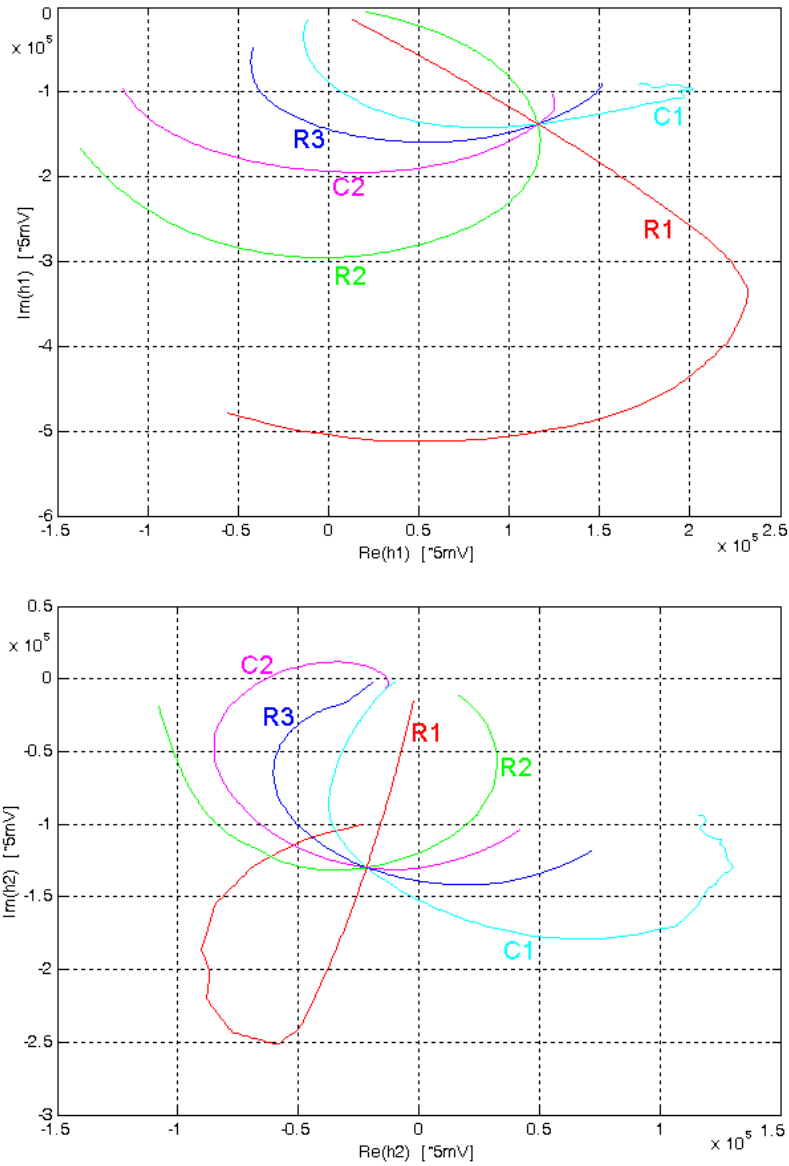
9

Figure 10. Families of localization curves generated for the APUT (Fig. 3) based on transformation (1)

This approach is derived from the generalized transformation presented in [14], which utilizes modified formulae of the DFT. Hence, the new generalized transformation for the m-th frequency component ($m = 1$, .., M) has the form:

$$h_{m,j,i}\left(p_{j,i}\right) = \sum_{n=1}^{N} v_{n,j,i}\left(p_{j,i}\right)\zeta^{m(n-1)} \qquad (1)$$

where $v_{n,j,i}(p_{j,i})$ − n-th voltage sample of the time response of the APUT for the j-th value of the i-th component, $\zeta = e^{-\varphi}$, $\varphi = \dfrac{2\pi\gamma}{N}$ and $\gamma^2 = -1$ [14].

That is, the i-th curve can be represented by the set of points with coordinates $\{\mathrm{Re}(h_{m,j,i}), \mathrm{Im}(h_{m,j,i})\}_{j=1,...,J}$ and $m=1,...,M$. To illustrate the method, we take into account only two first frequency components h_1 and h_2. It was $m = 1$ in [14]. Obviously, increasing the dimension of the measurement space increases the size of the

10

fault dictionary and computational time, but it improves the fault localization resolution [10,11]. Thus, in this case $K = 2m = 4$. Because it is difficult to present the four-dimensional space on the plane we depict it in the form of two separate planes, the first one for h_1 and the second one for h_2 (Fig. 10).

As mentioned in [14] we can write that $e^{-\gamma\alpha} = \cos\alpha + \gamma\sin\alpha$. Thus (1) can be transformed and divided into two formulas:

$$\text{Re}\, h_{m,j,i}\left(p_{j,i}\right) = \sum_{n=1}^{N} v_{n,j,i}\left(p_{j,i}\right)\cos\left(m\alpha(n-1)\right) \tag{2a}$$

$$\text{Im}\, h_{m,j,i}\left(p_{j,i}\right) = \sum_{n=1}^{N} v_{n,j,i}\left(p_{j,i}\right)\sin\left(m\alpha(n-1)\right) \tag{2b}$$

It is recommended to reduce the size of the program code. We can do it by using only one trigonometric function (for instance, cosines) in the program. Hence, basing on the fact that $\sin\alpha = \cos(\pi/2 - \alpha)$, where $\alpha = 2\pi/N$, we can change (2b) to the following form:

$$\text{Im}\, h_{m,j,i}\left(p_{j,i}\right) = \sum_{n=1}^{N} v_{n,j,i}\left(p_{j,i}\right)\cos\left(\frac{\pi}{2} - m\varphi(n-1)\right) \tag{3}$$

Thanks to this, we also obtain a simple code with implementation of transformations (2a) and (3) for $m = 2$, as shown in Listing 1.

```
#define N   32   // the number of voltage samples
#define M_PI  3.14159265358979323846264\3
#define PI_2  1.57079632679489661923132\1

volatile int16_t v[N], vp; // ADC results
double re_h, im_h, phi, phi_re, phi_im;
double re_h2,im_h2,phi2,phi_re2,phi_im2;
...
  phi = (-2*M_PI)/N;
  phi2 = 2.*phi;

  re_h = 0;
  im_h = 0;
  re_h2 = 0;
  im_h2 = 0;

  for(n=0;n<N;n++)
    {
```

11

```
    phi_re = phi*n;
    phi_im = PI_2 - phi_re;
    phi_re2 = phi2*n;
    phi_im2 = PI_2 - phi_re2;
    re_h += v[n]*cos2(phi_re);
    im_h += v[n]*cos2(phi_im);
    re_h2 += v[n]*cos2(phi_re2);
    im_h2 += v[n]*cos2(phi_im2);
    }
```

Listing 1.   Fragments of the program code with implementation of transformations (2a) and (3) written in ANSI C language for ATmega16

We also propose to replace the *cos* function, which needs 3387 MCU clocks to calculate the result of a double type [21], by its simple Maclaurin series equivalent (4). It is possible because during fault detection and localization we compare the measurement point and the fault dictionary both calculated in the same way, that is, based on the same transformation (1). Hence, the *cos* function has the form:

$$\cos(\alpha) = 1 - \frac{\alpha^2}{4} \quad \text{for} \quad \alpha \in \left\langle -\frac{\pi}{2}, \frac{\pi}{2} \right\rangle \tag{4}$$

and its code implementation is following:

```
double cos(double x)
{
double y,z;
char sign = 1;

while ( -PI_2 > x)
    {
    x += M_PI;
    sign *= (-1);
    }
while ( PI_2 < x)
    {
    x -= M_PI;
    sign *= (-1);
    }

z = (x*x)/4;
y = (1 - z)*sign;
return(y);
}
```

Listing 2.   The ANSI C code of the *cos* function based on (4)

Thanks to this, we shortened the computations made by the microcontroller about ten times, and we also reduced the size of the program code. The code of the measurement part consumes about 2.2 kB of the program memory. Hence, the calculations are relatively simple and they can be executed by 8-bit microcontrollers.

D. Selection of parameters of the fault diagnosis method

The duration time T of a stimulating square impulse, the acquisition time T_a and the number N of voltage samples should be established in a way enabling to obtain possibly the best localization resolution of the method by simultaneously maintaining optimal parameters such as the size of the fault dictionary and the duration time of the measurement procedure.

The way of determination of the duration time T is presented in [11]. The determination of the acquisition time T_a can be based on a threshold criterion. We know that the amplitude of the time response of the APUT diminishes in time. That is, the amount of information about the APUT included in the signal response also diminishes. Therefore, we can define the amplitude threshold ξV_{DD}, where $\xi \in (0,1)$. For instance, the time, after which the average value of amplitudes of considered time responses achieves this threshold, can be set as the acquisition time T_a. We established $T_a = 10T$.

The number N of voltage samples should be possibly the greatest [22]. But we have two limitations: small dimension of the internal data SRAM of the microcontroller, from tens of bytes to a few kilobytes (ATmega16 has 1024 bytes), and the minimum ADC conversion time. This time should be shorter than t_s, because the ADC has to be on time before the next conversion. From the spiADC timings (Fig. 7) and hardware properties [15,16] it follows that the full ADC conversion takes $3 \cdot (3 + 24 \cdot 2)/f_{osc}$, where $f_{osc} = 4$ MHz is the frequency of the system clock of the microcontroller, what gives about 14 µs plus the time needed for execution of the part of the code of the measurement function. Thus, we assumed $N = 32$.

E. The fault detection and localization procedures

Thanks to that we proposed the transformation (1), which allows to create the fault dictionary as a set of data describing a family of localization curves (Fig. 10), we can use the fault detection and localization procedures described in [10-13].

These procedures run according to the flow chart presented in Fig. 11.
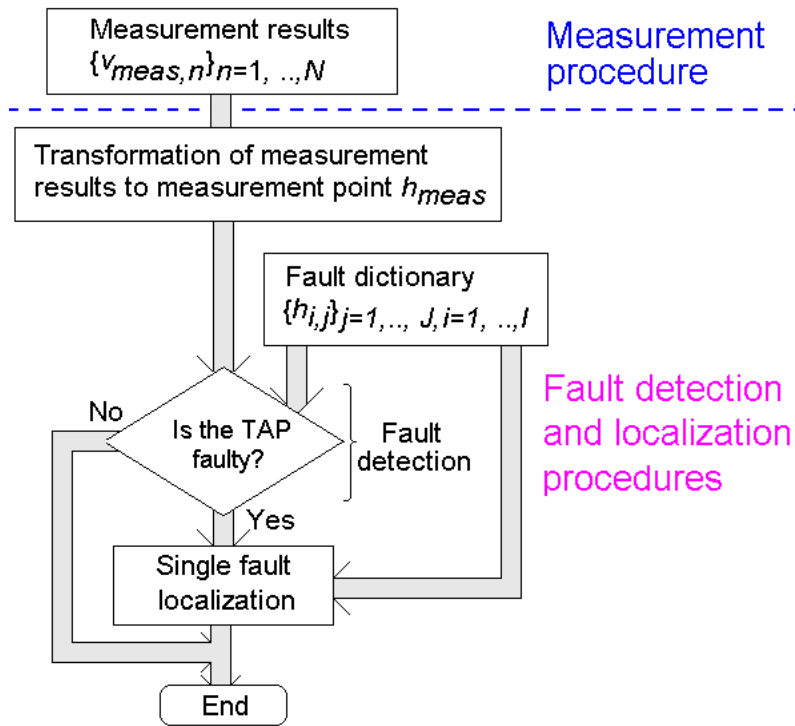
13

Figure 11. Fault detection and localization procedures

In the first step the N measured voltage samples $\{v_{meas,n}\}_{n=1,...,N}$ are transformed based on (2a) and (3) to the "measurement point". Next, we use the fault detection and localization procedures based on determination of the mutual position between the measurement point and localization curves [10-13].

During the fault detection procedure we check that the measurement point plotted in the measurement space is enclosed in the nominal area representing the nominal state of the APUT. If we detect a fault, we run the single soft fault localization procedure.

It can work according to two criteria elaborated by the author. In the first case [11], it checks on which curve or in the nearness of which curve the measurement point is placed. Hence, if the measurement point is situated nearest the i-th localization curve, it points that the p_i component is faulty. The second criterion [12] is dedicated for circuits, in which we take into account tolerances of non-faulty components. In this case localization curves become fuzzy and become localization belts. Thus, if the measurement point is situated inside the i-th localization belt, it indicates that the i-th component is faulty.

III. EXPERIMENTAL VERIFICATION

The new approach was experimentally verified on the example of the low-pass filter shown in Fig. 3. The operational amplifier LM358N of STMicroelectronics operates from a double power supply ($V_- = -9$ V, $V_+ = +9$ V). It is tested by the digital part represented by the ATmega16 (Fig. 2). It works with a 4 MHz quartz crystal oscillator. Timer 1 is clocked directly by the system clock. It is used to determine the sampling times of the ADC. Timer 0, clocked by the system clock with the prescaler divisor 8, generates at the output OC0

14

the stimulating square pulse with a duration time $T = 196$ µs. The amplitude of this signal on the SSC output is equal to $-V_{DD} = -5.0992$ V. The reference voltage of the AD7694 is set to $V_{DD} = V_{ref} = 5.0767$ V and verified by the HP34401A multimeter.

Measurements were carried out for 33 values of each element. One value was set to the nominal value and the 32 values were logarithmically located in the following ranges of element value changes: from 1540 Ω to 110.420 kΩ for R_1 and R_2, from 348 Ω to 34.810 kΩ for R_3, from 1.00 nF to 100.28 nF for C_1 and from 4.71 nF to 470.57 nF for C_2.

Different soft faults of each i-th component were physically entered to the APUT and each time the measurement procedure was run. For resistors, a decade resistor was used and for the capacitors a decade capacitor whose values were controlled by the precision E4980A LRC meter (Func. Cp-D, Freq. 1 kHz, Level 1 V, Bias 0 V). To verify the measurement procedure and correctness of work of the measurement microsystem, the four coordinates of the measurement point calculated by the microcontroller were sent to the personal computer via the RS232.

It allows to plot the measurement points in the form of triangles for R_1 and R_2, squares for R_3 and C_1 and circles for C_2 on the simulation curves (solid lines) in Fig. 12.

An example of experimental results is shown in Table 1. It only concerns the results of localization of the $C2$ component made by the fault localization algorithm based on the criterion proposed in [11]. Table 1 shows also coordinates of the respective measurement points and the symbol of the component qualified as faulty. From Table 1 it is seen that for this component all localization results are correct. For the nominal value (47.057 nF) of the C2 component the tested circuit is fault free, what was noted down by a "nominal" word.

Table 1. An example of experimental results of localization of the C2 component made by the fault localization algorithm.

C2 [nF]	Re h_1	Im h_1	Re h_2	Im h_2	localization result
	[* 5 mV * 10^5]				
4.71	1.2086	-1.0254	3.7421	-1.0409	C2
5.46	1.2116	-1.0304	3.6645	-1.0499	C2
6.33	1.2140	-1.0365	3.5987	-1.0580	C2
7.35	1.2165	-1.0422	3.5080	-1.0679	C2
8.52	1.2211	-1.0506	3.3884	-1.0816	C2
9.89	1.2220	-1.0573	3.2604	-1.0956	C2
11.47	1.2259	-1.0684	3.0876	-1.1129	C2
13.31	1.2278	-1.0803	2.8626	-1.1313	C2
15.44	1.2303	-1.0971	2.5928	-1.1545	C2
17.92	1.2340	-1.1144	2.2577	-1.1792	C2
20.79	1.2363	-1.1373	1.8432	-1.2074	C2
24.12	1.2369	-1.1657	1.2974	-1.2369	C2
27.98	1.2330	-1.1983	0.6673	-1.2660	C2
32.46	1.2198	-1.2897	-0.0452	-1.2897	C2
37.66	1.1985	-1.2884	-0.8681	-1.3037	C2
43.69	1.1620	-1.3508	-1.8401	-1.2984	C2
47.057	1.1402	-1.3861	-2.3756	-1.2889	**nominal**
50.69	1.1160	-1.4221	-2.9207	-1.2751	C2
58.80	1.0575	-1.4973	-4.1071	-1.2226	C2
68.22	0.9879	-1.5783	-5.2396	-1.1438	C2

79.15	0.9056	-1.6611	-6.3210	-1.0378	C2
91.82	0.7998	-1.7424	-7.2144	-0.9038	C2
106.53	0.6699	-1.8209	-7.9718	-0.7504	C2
123.59	0.5123	-1.8999	-8.5132	-0.5810	C2
143.38	0.3318	-1.9272	-8.5074	-0.3954	C2
166.35	0.1428	-1.9394	-8.0184	-0.2152	C2
192.99	-0.0637	-1.9193	-7.0492	-0.0558	C2
223.89	-0.2780	-1.8683	-5.7284	0.0610	C2
259.75	-0.4978	-1.7762	-4.2204	0.1263	C2
301.35	-0.7086	-1.6357	-2.7999	0.1211	C2
349.62	-0.8978	-1.4515	-1.7065	0.0711	C2
405.61	-1.0440	-1.2227	-1.2411	0.0006	C2
470.57	-1.1394	-0.9536	-1.2762	-0.0062	C2

Comparing the placement of the measurement points with theoretical curves in Fig. 12 it is seen that these points are situated on their curves, what experimental confirms that the method works correctly. Only for small values of R_1 and C_1 there are divergences, which however do not influence the correctness of the fault localization. These differences follow from the fact that for these values the APUT response exceeds the voltage range of correct work of the amplifier (Fig. 13). In this case the amplifier is overdriven. Thus, taking into account this fact, we supplemented the model of the APUT used in the MATLAB simulation. The modified parts of curves for R_1 and C_1 components are presented as dotted lines in Fig. 12.
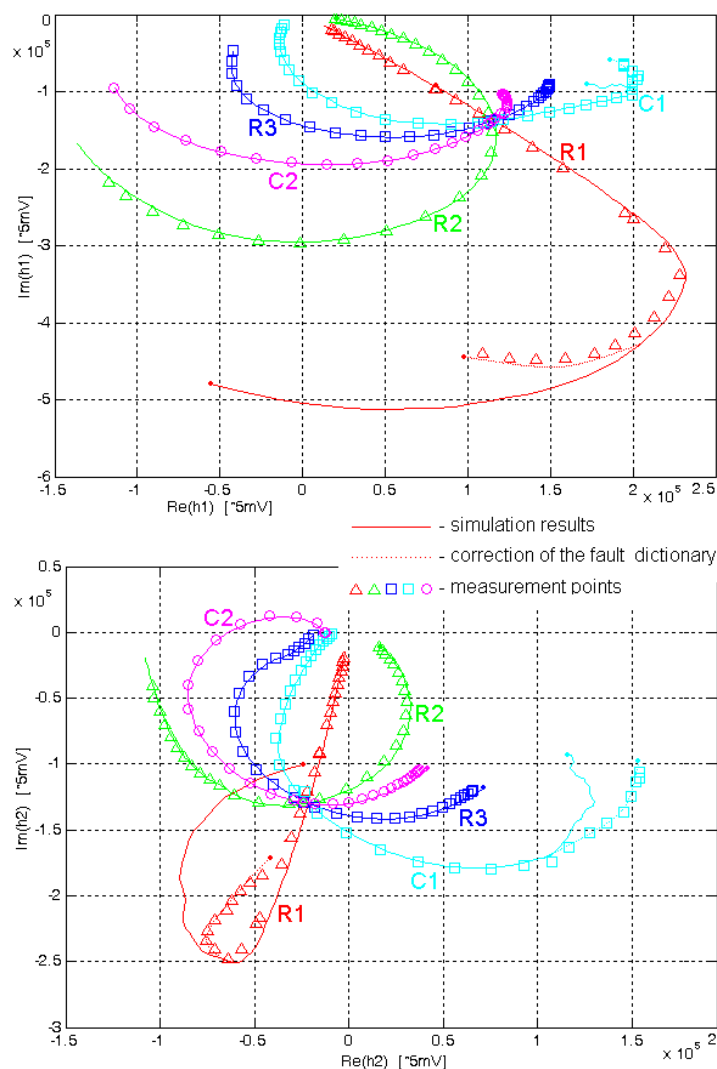

Figure 12. Families of localization curves generated for the APUT (Fig. 3) based on transformation (1)
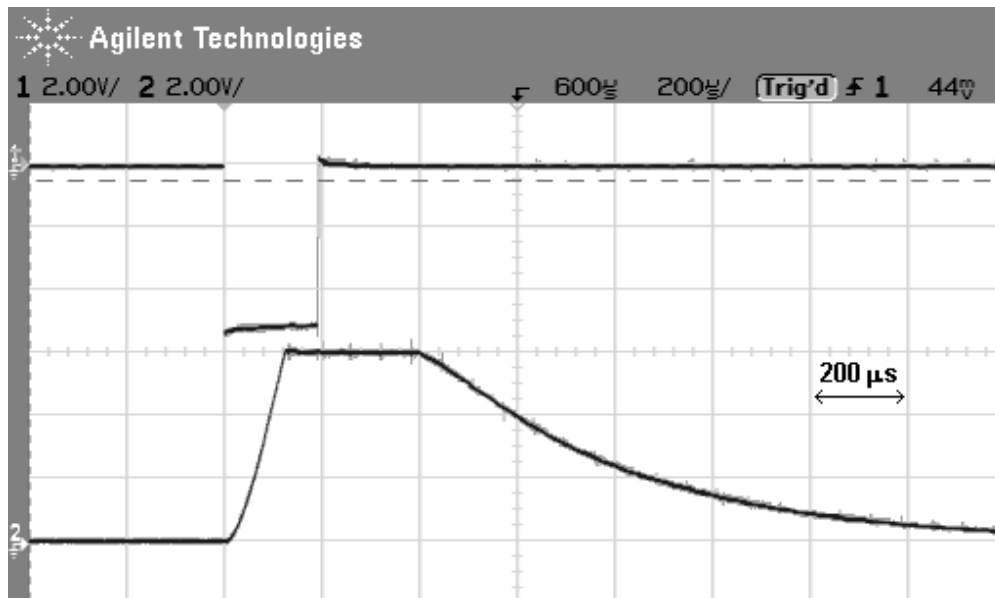
16

Figure 13. Timings of the stimulation square impulse and the time response of the APUT for $R_1 = 2\ k\Omega$
(observed by the 54622D oscilloscope)

IV. CONCLUSIONS

A new approach to self-testing of an analog part terminated by the ADC of mixed-signal electronic microsystems controlled by microcontrollers and its application and experimental verification are presented in the paper. The approach is based upon a new fault diagnosis method, for which the time response of the tested analog part to a single square pulse generated by the microcontroller is sampled many times by the external ADC in equal time intervals, and next this set of voltage samples is converted to the measurement point using the new transformation based on modified DFT formulae. The measurement procedure is realized by components already existing in the system i.e. the microcontroller (its timers and SPI interface) and the ADC. Also, the fault detection and localization procedures based on comparison of the measurement point with the fault dictionary placed in the microcontroller program memory are executed by the microcontroller. Thanks to this, this solution considerably decreases costs of testing of the analog part.

The small size of the fault dictionary and reasonable requirements of the method on the operating memory and the computing power allow to implement the self-testing approach in systems controlled by simple 8-bit microcontrollers.

Summarizing, the above-mentioned advantages give the possibility to use the presented approach in practice for testing or self-testing of analog parts of mixed-signal electronic embedded systems controlled by microcontrollers or by signal processors.

REFERENCES

[1] Zhao F., Koutsoukos X., Haussecker H., Reich J., Cheung P., "Monitoring and fault diagnosis of hybrid systems", IEEE Transactions on Systems, Man, and Cybernetics—Part B: Cybernetics, vol. 35, 2005, pp. 1214-1219.

[2] Scottow R. G., Hopkins A. B. T., "Instrumentation of real-time embedded system for performance analysis", IEEE Instrumentation and Measurement Conference, IMTC/06, Sorrento, Italy, 2006, pp.1307-1310.

[3] Changhyun B., Seungkyu P., Kyunghee C., "[similar to] TEST: An effective automation tool for testing embedded software", WSEAS Transactions on Information Science and Applications, vol. 2, 2005, pp. 1214-1219.

[4] Souza C. P., Assis F. M., Freire R. C. S., "Mixed test pattern generation using single parallel LFSR", IEEE Instrumentation and Measurement Conference, IMTC/06, Sorrento, Italy, 2006, pp. 1114-1118.

[5] Raczkowycz J., Mather P., Saine S., "Using a sigma-delta modulator as a test vehicle for embedded mixed-signal test", Microelectronic Journal, vol. 31, issue 8, 2000, pp. 689-699.

[6] Prenat G., Mir S., Vazques D., Rolindez L., "A low-cost digital frequency testing approach for mixed-signal devices using $\Sigma\Delta$ modulation", Microelectronic Journal, vol. 36, issue 12, 2005, pp. 1080-1090.

[7] Toczek W., Zielonko R., "A measuring systems for fault detection via oscillation", XVI IMEKO World Congress, Vienna, Austria, 2000, vol. 6, pp. 287-292.

[8] Toczek W., "Analog fault signature based on sigma-delta modulation and oscillation - test methodology", Metrology and Measurement Systems, vol. XI, No. 4, 2004, pp. 363-375.

[9] Negreiros M., Carro L., Susin A. A., "Testing analog circuits using spectral analysis", Microelectronic Journal, vol. 34, issue 10, 2003, pp. 937-944.

[10] Z. Czaja, "Using a square-wave signal for fault diagnosis of analog parts of mixed-signal electronic embedded systems", IEEE Transactions on Instrumentation and Measurement, vol. 57, 2008, pp. 1589-1595.

[11] Czaja Z., "A diagnosis method of analog parts of mixed-signal systems controlled by microcontrollers", Measurement, vol. 40, 2007, pp. 158-170.

[12] Czaja Z., "A method of fault diagnosis of analog parts of electronic embedded systems with tolerances", Measurement, vol. 42, 2009, pp. 903-915.

[13] Toczek W., Czaja Z., "Diagnosis of fully differential circuits based on a fault dictionary implemented in the microcontroller systems", Microelectronics Reliability, vo. 51, issue 8, 2011, pp. 1413-1421.

[14] Czaja Z., „ Self-testing of analog parts of mixed-signal electronic microsystems based on multiple sampling of time responses", IEEE Instrumentation and Measurement Conference, I2MTC/2012, Graz, Austria, 2012, pp. 477-482.

[15] Atmel Corporation, "8-bit AVR microcontroller with 16k Bytes In-System Programmable Flash, ATmega16, ATmega16L", 2006, PDF file available from: www.atmel.com.

[16] Analog Devices, "AD7694, 16-Bit, 250 kSPS PulSAR® ADC in MSOP", 2005, PDF file available from: www.analog.com

[17] International Rectifier, "IRF7105 HEXFET Power MOSFET, 2003, PDF file available from: www.irf.com.

[18] F. Reverter, O. Casas, "Direct interface circuit for capacitive humidity sensors", Sensors and Actuators A, vol. 143, 2008, pp. 315–322.

[19] F. Reverter, J. Jordana, M. Gasulla, R. Pallàs -Areny, "Accuracy and resolution of direct resistive sensor-to-microcontroller interfaces", Sensors and Actuators A, vol. 121, 2005, pp. 78–87.

[20] F. Reverter, O. Casas, "Interfacing Differential Capacitive Sensors to Microcontrollers: A Direct Approach, IEEE Transactions on Instrumentation and Measurement", vol. 59, no. 10, 2010, pp. 2763-2769.

[21] "avr-libc 1.6.7", avr-libc-user-manual.pdf file, Generated by Doxygen 1.5.6, 2010.

[22] Watkinson J., "The art of digital audio", Third Edition, Elsevier, 2001.